Digital map and probability compensation model for repeated positioning error of feed axis

Huayang Wu
Dunwen Zuo (imit505@nuaa.edu.cn)
Nanjing University of Aeronautics and Astronautics

Research Article

Keywords: feed axis, repeated positioning error, error digital map, dynamic optimization, error probability modeling

Posted Date: August 4th, 2022

DOI: https://doi.org/10.21203/rs.3.rs-1903562/v1

Digital map and probability compensation model for repeated positioning error of feed axis

Huayang Wu[1], Dunwen Zuo[1*]

1College of Mechanical and Electrical Engineering, Nanjing University of Aeronautics and Astronautics, Nanjing, China

*Correspondent author. Telephone:025-84890249

E-mail address: imit505@nuaa.edu.cn

Abstract: The randomness of the repeated positioning error of feed shaft is the main reason for the difficulty to address this error. The previous repeated loading and unloading suppression methods will easily do damages to parts. This paper sets out to investigate the probability distribution of all possible error values while feed shaft is at different positions, and determine the maximum value of probability error from the random errors. With feed axis at a certain position, first of all, we count the probability of each error based on a large number of random errors. We also draw the digital map of the repeated positioning error of this error with the error of positive and negative stroke measurement as the x-axis and y-axis coordinates and the probability of each error value as the z-axis coordinates Secondly, based on the digital map of each position on the feed axis and combined with the dynamic optimization algorithm, we find the highest point on the map and take the coordinate point of this point as the starting point of each position compensation. Then, we set the error probability threshold to control the possibility of compensation errors and output the size and direction of the final compensation value. Finally, we start the compensation command and detect the compensated error. The error data that fail to meet the requirements will enter the probability statistics again, redraw the digital map and update the map. Through real-time detection and feedback, the digital map is dynamically improved to adapt to the changing environment. This probability compensation model of repeated positioning error can end the suppressing repeated positioning errors brought by repeatedly disassembling parts.

Keywords: feed axis, repeated positioning error, error digital map, dynamic optimization, error probability modeling

Highlights

1. A description method of repeated positioning error of feed shaft is proposed.
2. The probability compensation model of repeated positioning error of feed shaft is constructed.
3. A dynamic modeling method of probability compensation model for repeated positioning error is described.

Acknowledgements

It is great thankful to NEWAY CNC EQUIPMENT（SUZHOU）CO., LTD for providing experimental instruments.

Digital map and probability compensation model for repeated positioning error of feed axis

Huayang Wu[1], Dunwen Zuo[1*]
1College of Mechanical and Electrical Engineering, Nanjing University of Aeronautics and Astronautics, Nanjing, China
*Correspondent author. Telephone:025-84890249
E-mail address: imit505@nuaa.edu.cn

Abstract: The randomness of the repeated positioning error of feed shaft is the main reason for the difficulty to address this error. The previous repeated loading and unloading suppression methods will easily do damages to parts. This paper sets out to investigate the probability distribution of all possible error values while feed shaft is at different positions, and determine the maximum value of probability error from the random errors. With feed axis at a certain position, first of all, we count the probability of each error based on a large number of random errors. We also draw the digital map of the repeated positioning error of this error with the error of positive and negative stroke measurement as the x-axis and y-axis coordinates and the probability of each error value as the z-axis coordinates Secondly, based on the digital map of each position on the feed axis and combined with the dynamic optimization algorithm, we find the highest point on the map and take the coordinate point of this point as the starting point of each position compensation. Then, we set the error probability threshold to control the possibility of compensation errors and output the size and direction of the final compensation value. Finally, we start the compensation command and detect the compensated error. The error data that fail to meet the requirements will enter the probability statistics again, redraw the digital map and update the map. Through real-time detection and feedback, the digital map is dynamically improved to adapt to the changing environment. This probability compensation model of repeated positioning error can end the suppressing repeated positioning errors brought by repeatedly disassembling parts.

Keywords: feed axis, repeated positioning error, error digital map, dynamic optimization, error probability modeling

1.Introduction

Precision machine tools, which can process a variety of precision parts such as boxes and disks are widely used in military and civil industries. The feed shaft is the core transmission part of the machine tool [1], and the repeated positioning error of the feed shaft is one of the important indexes for the evaluation of machine tool. The requirements for precision machine tools are high speed, high precision and high repeatability [2,3]. However, the randomness of the repeated positioning error of the linear axis makes it unable to build a model similar to deterministic compensation model of the positioning error. Thus, there is an urgent need for precision to reduce the repeated position error of feed shaft.

At present, there is little theoretical analysis on the repeated positioning error of the feed shaft, most of which focus on the experimental study of the influencing factors to the repeated positioning error, or reducing the repeated positioning error through the modeling and suppression of assembly

error. Sun et al. [4] conducted experimental research on the mechanism of the repeated positioning error of the feed axis of the NC machine tool, determining the factors affecting the repeated positioning error of the feed axis through orthogonal experiments and proposing an assembly method to reduce the repeated positioning error of the feed axis. Szipka et al. [5] proposed a method for determining the repeatability of non-uniform parameters in the workspace under static and no-load conditions. They also made a detailed description of the multiaxial repeatability performance, which contributes to the understanding the root causes of performance changes in the manufacturing process. Mori et al. [6] also proposed a method of design and formation of workforce skills for machine tool assembly using simulations . They developed a simulation model based on the investigation of the actual machine tool workshop and applied several forms of labor skills into simulation. Considering the influence of joint surface deformation, Lu et al. [7] established a hybrid genetic algorithm and back-propagation neural network model to predict the assembly changes caused by joint surface deformation under different assembly conditions and parameters. Wang et al. [8] put forth an assembly performance method. called pre-deformation. Since this method is technically based on machine tool assembly and collaborative computer aided engineering (CAE) analysis, it helps increase the assembly performance. He et al. [9] studied the propagation of machine tool changes caused by geometric errors during assembly and used the state space model to describe the change propagation in the process of machine tool assembly. This method has strong feasibility and practicality. Sun et al. [10] studied the influence of geometric errors on the repeatability of linear axis positioning, and proposed a mathematical model between the geometric errors of moving parts and the motion posture. Based on genetic algorithm, they determined the influence of geometric error on the repeatability of linear axis positioning. Due to the complexity of the repeated positioning error, most scholars attempt to make a breakthrough on the positioning error of the feed shaft such as thermal error. For example, models, such as neural network modeling, dynamic modeling and finite element modeling [11-15], can accurately predict the positioning error of feed shaft, but these modeling methods are not well applied to reduce the repeated positioning error of the feed shaft. Based on the previous research, it is found that the lack of model of repeated positioning error model leads to a single means of restraining repeated positioning error. Usually, it exploits the experimental method to determine the possible influencing factors of repeated positioning error (such as preload and assembly accuracy) and the influence size of each factor, and makes adjustments by dissembling parts according to the experimental results.

The adjustment of assembly sequence can reduce the repeated positioning error to a certain extent. However, with the use times of the machine tool growing, each part of the machine tool will change. Then, parts must be disassembled and assembled again to adapt to the new changes. This method of repeated assembly is of blindness, which does allow researchers to fully grasp the distribution law of errors. In addition, repeated disassembly and assembly is very easy to damage parts [16]. In view of the above problems, this paper makes analyses from the direction of experimental measurement, data modeling and error compensation. It also uses the measured data to build a digital map of repeated positioning error, and combines the dynamic optimization algorithm to build a probability compensation model of repeated positioning error of the feed shaft and test the error compensation. The method of error probability compensation can efficiently eliminate the disadvantages brought by repeatedly disassembling parts. The model construction process is shown in the **Fig. 1**.

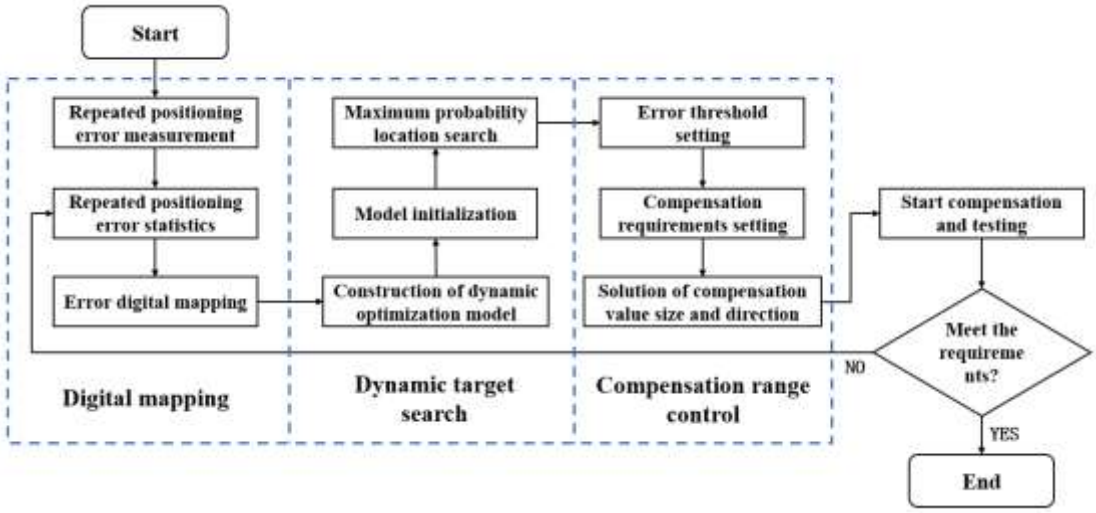

Fig. 1. Flow chart of repeated positioning error probability compensation model

2. Digital map drawing of repeated positioning error

The key to constructing probability compensation model is to draw the digital map of repeated positioning error. Based on a large number of repeated positioning error data, we found the frequency of some error at a certain position, and further calculated the probability of this error. The digital map of repeated positioning error is drawn using the statistical probability distribution of the positive and negative direction error of the feed axis, and the drawing method is shown in **Fig. 2**.

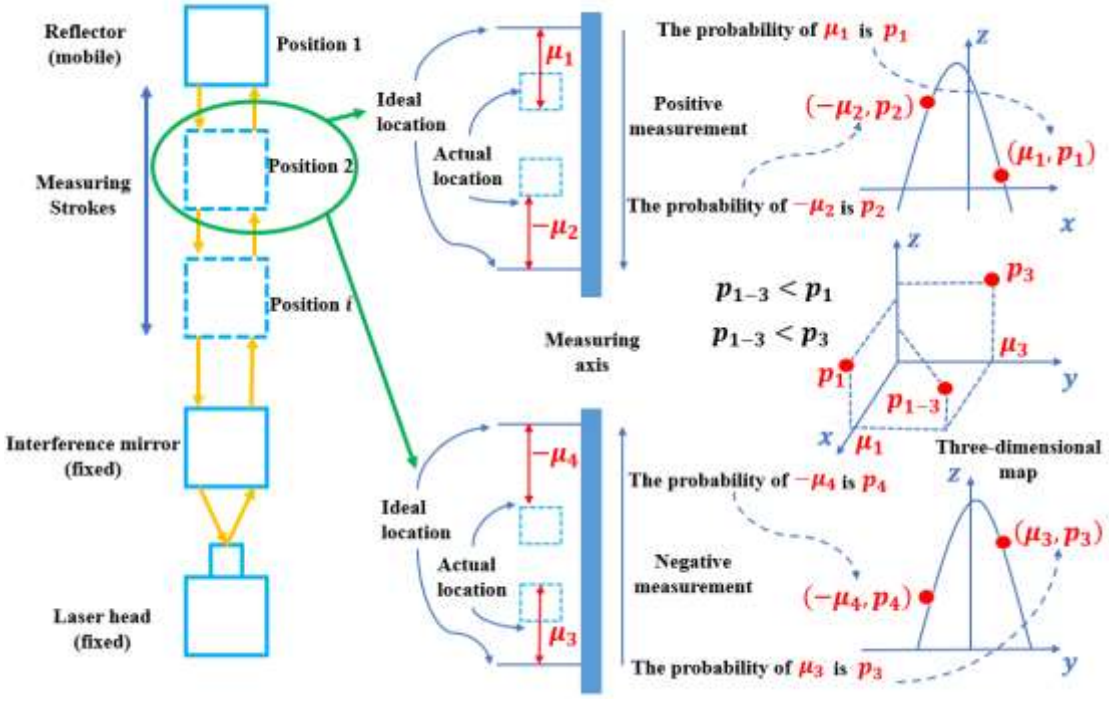

Fig. 2. Construction process of digital map of repeated positioning error

The construction process of repeated positioning error digital map has the following steps：

Step 1, arrange the laser interferometer according to the measurement position;

Step 2, move the feed shaft to drive the reflector;

Step 3, use the position of the mirror to measure the error of the feed axis;

Step 4, repeat step 2 and step 3 for N times, and record the measurement error value of each time;

Step 5, count the error distribution frequency of each position of positive stroke and negative stroke according to the recorded measurement error value;

Step 6, calculate the error distribution probability of each position according to the error distribution frequency of each position;

Step 7, build the coordinate axis of the specific location digital map. Among them, x-axis coordinate represents the positive stroke error value of the position, y-axis represents the negative stroke error value of the position, and z-axis represents the probability of taking the error value;

Step 8, draw a digital map of the repeated positioning error of each position.

In order to obtain a complete digital map, it is necessary to draw three-dimensional points outside the coordinate axis. Nonetheless, this point is of no practical significance. To ensure that the data points outside the coordinate axis do not affect the search results, as shown in **Fig. 2**, the following conditions should be met:

$$p_{1-3} < p_1 \tag{1}$$

$$p_{1-3} < p_3 \tag{2}$$

Where $p_{1\text{-}3}$ represents the probability of error points outside the coordinate axis, and p_1 and p_3 represent the probability of error points on the coordinate axis.

The x-axis and y-axis represented by the positive stroke and negative stroke intersect at the origin, and the corresponding z-coordinate value takes the maximum value of the x-axis and y-axis at the intersection. It will be mentioned in the later analysis that the origin corresponds to no compensation, and taking the maximum probability of positive and negative stroke 0 error at the origin can reduce the probability of error compensation.

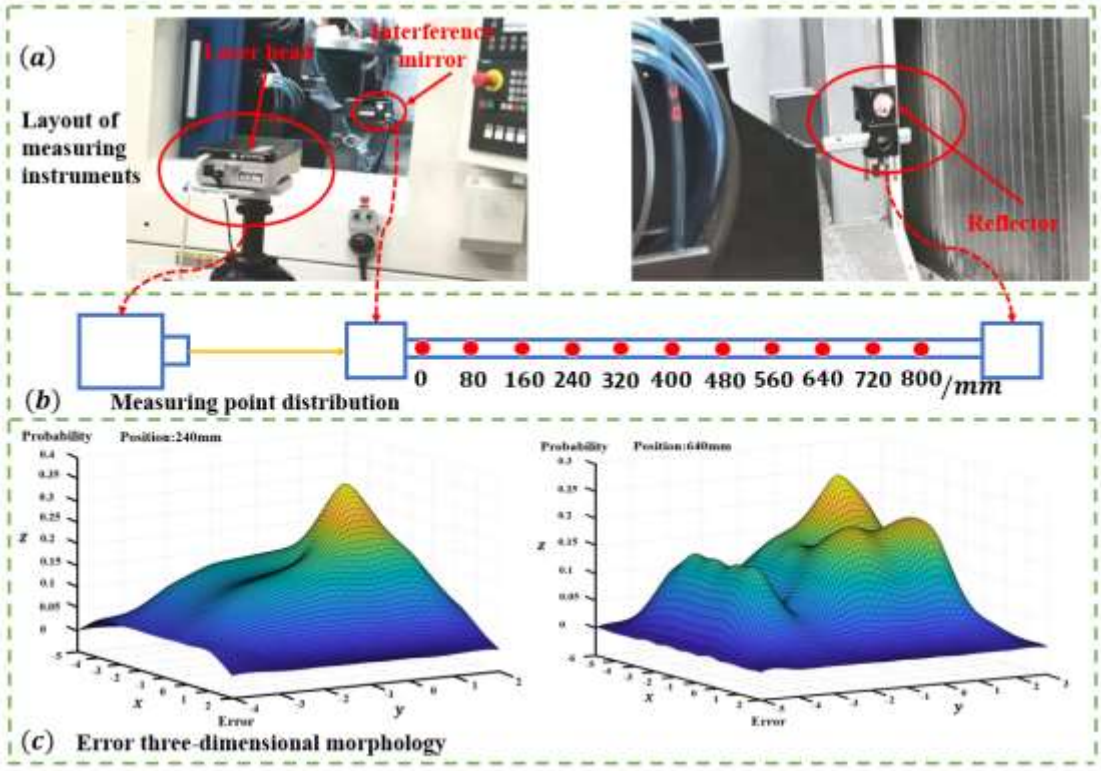

Fig. 3. Repeated positioning error measurement and digital map drawing of feed axis

As shown in **Fig. 3** (a) and **Fig. 3** (b), the object of this digital map drawing is the feed axis of

the horizontal CNC machining center, and a total of 11 digital maps are drawn. Among them, the digital map of 240 mm position and 640 mm position is shown in **Fig. 3** (c). As for the x-axis and y-axis in **Fig. 3** (c), a negative value represents that the actual motion fails to reach the ideal point, a positive value represents that the actual motion exceeds the ideal point, and 0 represents that the actual motion just reaches the ideal point. The Z-axis in **Fig. 3** (c) represents the probability of taking the error value. After comparing the two digital maps, it can be seen that the morphology of maps at different locations varies greatly, which may be single peak morphology or multi peak morphology. These conditions also reflect that the probability distribution of repeated positioning error at each position differs.

The digital map at 240 mm was extracted for further analysis. As shown in **Fig. 4** and **Fig. 5**, there are also significant differences in the probability distribution of positive travel error and negative travel error at the same position, and the positions where the maximum probability occurs are also different. It shows that it is of necessity to place the positive and negative travel repeated positioning errors on different coordinate axes since it ensures that the probability distributions of the two direction errors will not mutually influence.

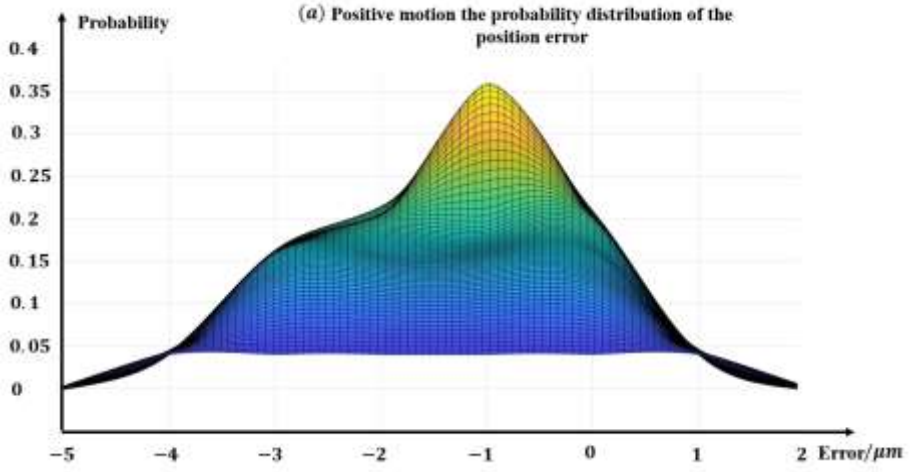

Fig. 4 Probability distribution of 240 mm positive motion error at position

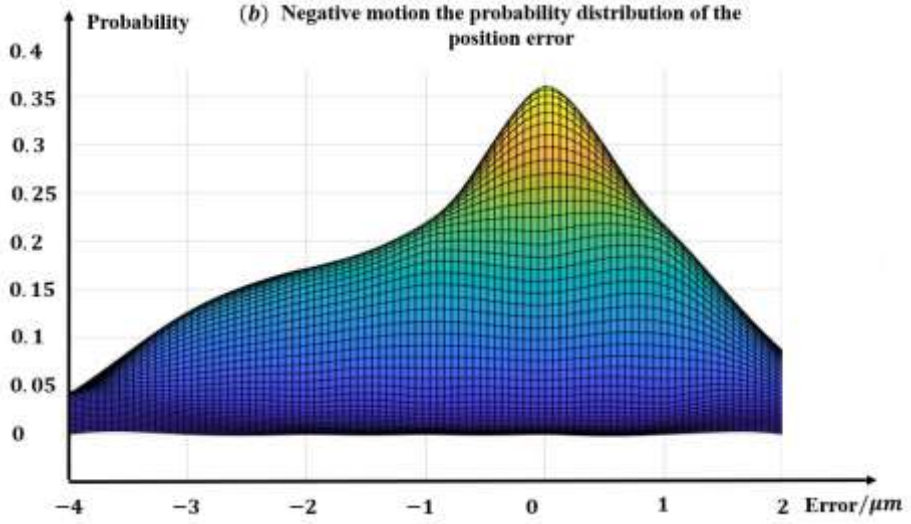

Fig. 5 Probability distribution of negative motion error at 240 mm position

The map shape is determined by the error probability of each position. Draw a digital map of the repeated positioning error of each position of the feed axis to form a map database for subsequent

calls.

3. Construction of probability compensation model for repeated positioning error

In actual processing, the position of the feed shaft is constantly changing, and the digital map of different positions is also different, which demands that the search environment should change constantly. Also, the target value of search is also changing continuously. It can be seen that this is a dynamic optimization problem. This paper addresses this problem through the dynamic particle swarm optimization algorithm based on sensitive particles. The flow of the dynamic particle swarm optimization algorithm based on sensitive particles is shown in **Fig. 6**.

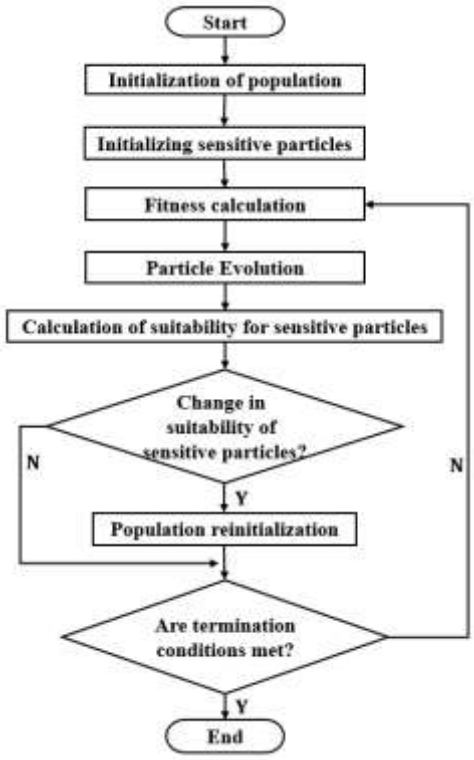

Fig. 6 Flow chart of dynamic particle swarm optimization algorithm based on sensitive particles

The fitness function of dynamic particle swarm optimization algorithm is:

$$fitness(x, y) = h(x, y) \tag{3}$$

Where h(x, y) is the height of the digital map of repeated positioning error.

Combined with the digital map obtained, the search process of the dynamic optimization algorithm is described in detail in **Fig. 7**. The change curve in **Fig. 7** illuminates the sum of the fitness of position sensitive particles in the positive stroke of feed shaft. In each iteration step, the x-axis coordinates and y-axis coordinates of sensitive particles remain unchanged, and whether the map changes are judged according to the sum of z-axis coordinates of all sensitive particles, namely fitness sum. If the map is not changed, the search process will be skipped, and the optimal value is the results of last search. If the map changes, the ordinary particles will be reinitialized, and the optimal value will be obtained according to the standard particle swarm search process. All particles will approach the particles with high fitness until all reach the optimal position.

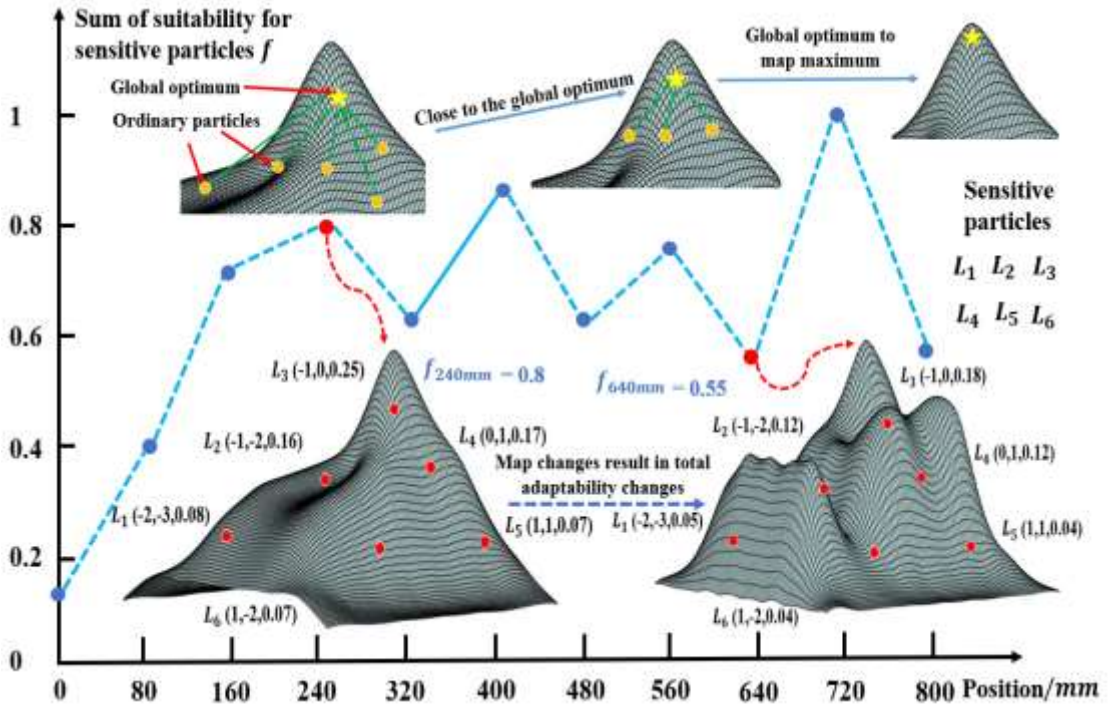

Fig. 7. Schematic diagram of dynamic optimization based on sensitive particle

Using the digital map of the repeated positioning error of the 11 positions of the feed axis, combined with the dynamic particle swarm optimization algorithm, the compensation points (i.e., the maximum probability point or the optimal value point) of the positive and negative strokes of each position of the feed axis are obtained, as shown in **Fig. 9** (a).

The size of the compensation value needs to be set before compensation, and the size of the compensation value depends on the compensation target. The compensation target of this study is that the repeated positioning error after compensation is between ± 1 μm. Since the probability compensation model provided in this paper has probability compensation errors and if the compensation direction is opposite or the error, the compensation will exceed the compensation target, there is a need to control the error probability of compensation. The control error probability of this model is less than 20%. Combined with **Fig. 4**, **Fig. 5** and **Fig. 9** (a), the specific process of determining the compensation value is as follows. The error probability distribution of positive and negative stroke can be obtained from the measured data of each position. In order to explain the compensation method concisely and clearly, only part of the position error probability distribution is listed.

Position 0 mm: Positive and negative compensation points are 0 μm, without compensation.

Position 80 mm: Positive and negative compensation points are 0 μm, without compensation.

Position 160 mm: Positive compensation point is -1 μm, and negative compensation point is 1 μm. The positive direction compensation is 1 μm, and the error rate is 4%. The negative direction is compensated by 1 μm, and the error rate is 48%, so the negative direction is not compensated. The difference probability distribution is shown in **Table 1** and **Table 2.**

Table 1 Probability distribution of positive repeated positioning error at 160mm position

Positive probability	0	4%	6%	12%	54%	20%	4%	0
Error point	-5	-4	-3	-2	-1	0	1	2

Table 2 Probability distribution of negative repeated positioning error at 160mm position

Positive probability	0	12%	16%	20%	20%	24%	8%
Error point	-4	-3	-2	-1	0	1	2

Position 240 mm: Positive compensation point is -1 μm, positive compensation is 1 μm, and error rate is 0. The negative compensation point is -1 μm, the negative compensation is 1 μm, and the error rate is 18%.

Position 320 mm: Positive compensation point is -3 μm. If the direct positive compensation is 3 μm, the error rate is 40%, and if the compensation is 2 μm, the error rate is 22%, so the compensation is 1 μm, and the error rate is 4%. The forward compensation 1 μm command is executed according to the threshold of out of tolerance probability. The negative compensation point is 0 μm. Thus, the negative direction is not compensated. The positive error distribution is shown in **Table 3**.

Table 3 Probability distribution of positive repeated positioning error at 320mm position

Positive probability	0	4%	4%	28%	24%	18%	18%	4%
Error point	-6	-5	-4	-3	-2	-1	0	1

Position 400 mm: Positive compensation point is -2 μm, positive compensation is 2 μm, and error rate is 20%. Negative compensation point is -1 μm, negative compensation is 1 μm, error rate is 4%.

Position 480 mm: Positive compensation point is -1 μm, positive compensation is 1 μm, and error rate is 16%. Negative compensation point is -1 μm, and the error rate of negative compensation of 1 μm is 44%. Hence, the negative direction is not compensated.

Position 560 mm: Positive compensation point is -1 μm, positive compensation is 1 μm, and error rate is 18%. Negative compensation point is -1 μm, negative compensation is 1 μm, and error rate is 18%.

Position 640 mm: Positive compensation point is -3 μm, positive compensation error rate of 3 μm is 40%, and compensation error rate of 2 μm is 20%. Therefore, compensation is 2 μm. The negative compensation point is -1 μm, the negative compensation is 1 μm, and the error rate is 14%.

Position 720 mm: Positive compensation point is -1 μm, positive compensation is 1 μm, and error rate is 4%. Negative compensation point is -2 μm, negative compensation is 2 μm, and error rate is 16%.

Position 800 mm: Positive compensation point is -2 μm, and if positive compensation is 2 μm, error rate is 24%. If the compensation is 1 μm and error rate is 5%, positive compensation will be 1 μm. If the negative compensation point is -3 μm and the negative compensation is 3 μm, error rate is 48%; if the compensation is 2 μm, error rate is 28%; if the compensation is 1 μm, error rate is 12%. Thus, the negative compensation is 1 μm.

The compensation direction and compensation value of each position are shown in **Fig. 8** and the probability of compensation out of tolerance at each position is counted, as shown in **Fig. 9** (b).

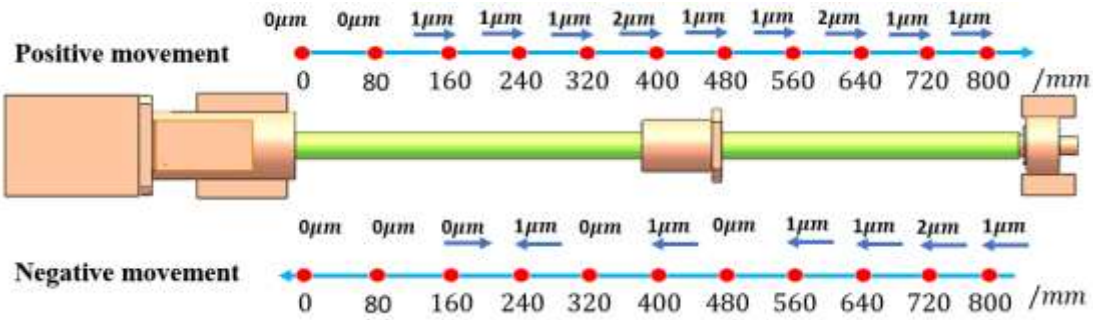

Fig. 8. Size and direction of measurement position compensation value

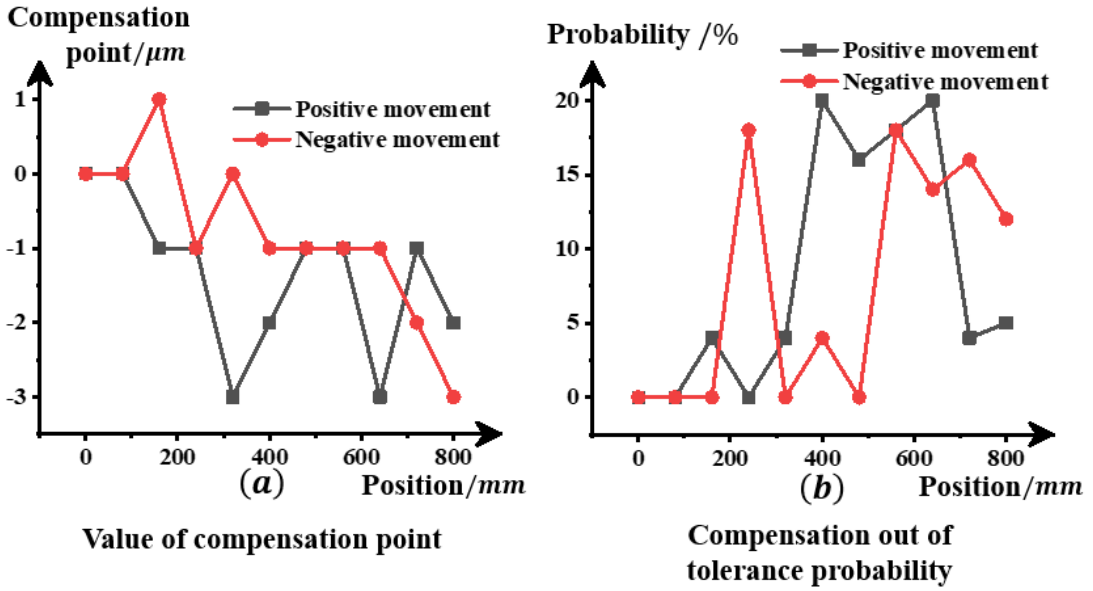

Fig. 9. Compensation points position and error probability

4. Application of probability compensation model

We have obtained a probability compensation model under specific working conditions through the above analysis, which includes the size and direction of compensation value. However, in the process of practical application, the working conditions are constantly changing, that is, the error probability distribution of each position is constantly changing, which requires a digital map model base covering all working conditions. Moreover, different processing requirements make different requirements for the range of repeated positioning error, which requires that the model can adapt to the adjustment of error probability threshold and error range. Combined with the previous analysis, a self-learning modeling method for the probability compensation model of repeated positioning error is proposed, as shown in **Fig. 10**. The so-called "self-learning" refers to that the new repeated positioning error can participate in digital map rendering and update the digital map model library in real time.

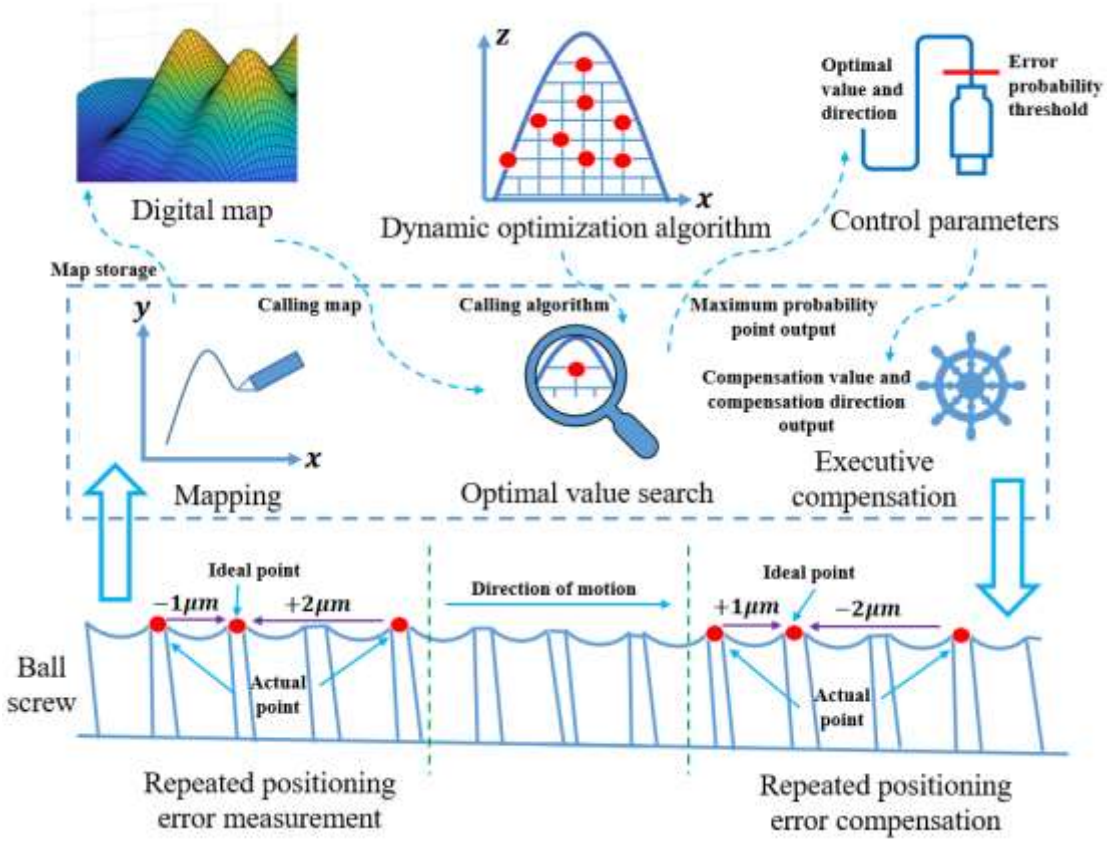

Fig. 10. Modeling and application of probability compensation model

In order to examine the practical applicational effect of the model, the previously obtained probability compensation model is detected by another five groups of repeated positioning error data. The first group of data used for error detection is shown in **Table 4**.

Table 4 Test data of the first group of models

Measuring point (mm)	0	80	160	240	320	400	480	560	640	720	800
Positive stroke error (μm)	0	0	-2	-1	-3	-3	-1	-2	-3	-3	-2
Negative stroke error (μm)	0	0	1	1	0	-1	0	0	-1	-2	-2

The compensation data shown in **Fig. 8** was applied to the error data in the **Table 4**. The compensation process and results are as follows.

Positive stroke error compensation process:

Position 0 mm: actual error is 0 μm, and compensation is 0 μm;

Position 80 mm: actual error is 0 μm, and compensation is 0 μm;

Position 160 mm: the actual error is -2 μm, the positive direction compensation is 1 μm, the reduced error is 1 μm, and the error after compensation is -1 μm;

Position 240 mm: the actual error is -1 μm, the positive direction compensation is 1 μm, the reduced error is 1 μm, and the error after compensation is 0 μm;

Position 320 mm: the actual error is -3 μm, the positive direction compensation is 1 μm, the reduced error is 1 μm, and the error after compensation is -2 μm;

Position 400 mm: the actual error is -3 μm, the positive direction compensation is 2 μm, the reduced error is 2 μm, and the error after compensation is -1 μm;

Position 480 mm: the actual error is -1 μm, the positive direction compensation is 1 μm, the reduced error is 1 μm, and the error after compensation is 0 μm;

Position 560 mm: the actual error is -2 μm, the positive direction compensation is 1 μm, the reduced error is 1 μm, and the error after compensation is -1 μm;

Position 640 mm: the actual error is -3 μm, the positive direction compensation is 2 μm, the reduced error is 2 μm, and the error after compensation is -1 μm;

Position 720 mm: the actual error is -3 μm, the positive direction compensation is 1 μm, the reduced error is 1 μm, and the error after compensation is -2 μm, which exceeded the maximum preset error;

Position 800 mm: the actual error is -2 μm, the positive direction compensation is 1 μm, the reduced error is 1 μm, and the error after compensation is -1 μm.

Negative stroke error compensation process:

Position 0 mm: actual error is 0 μm, and compensation is 0 μm;

Position 80 mm: actual error is 0 μm, and compensation is 0 μm;

Position 160 mm: actual error is 1 μm, and compensation is 0 μm;

Position 240 mm: actual error is 1 μm, the negative direction compensation is 1 μm, the increased error is 1 μm, and the compensated error is 2 μm, exceeding the maximum preset error;

Position 320 mm: actual error is 0 μm, and compensation is 0 μm;

Position 400 mm: actual error is -1 μm, the negative direction is compensated by 1 μm, the error is reduced by 1 μm, and the error after compensation is 0 μm;

Position 480 mm: actual error is 0 μm, and compensation is 0 μm;

Position 560 mm: actual error is 0 μm, the negative direction is compensated by 1 μm, the error is increased by 1 μm, and the error after compensation is 1 μm;

Position 640 mm: actual error is -1 μm, the negative direction is compensated by 1 μm, the error is reduced by 1 μm, and the error after compensation is 0 μm;

Position 720 mm: actual error is -2 μm, the negative direction is compensated by 2 μm, the error is reduced by 2 μm, and the error after compensation is 0 μm;

Position 800 mm: actual error is -2 μm, the negative direction is compensated by 1 μm, the error is reduced by 1 μm, and the error after compensation is -1 μm.

Based on the above analysis, a group of positive and negative stroke includes 22 measurement data in total, and the compensation command is started 15 times. The original data has a total error of 28 μm. After compensation, the error is reduced by 16 μm, accounting for 57% of the total error. After compensation, the error is increased by 2 μm, accounting for 7% of the total. Among them, there is a rise of error in the negative stroke position 240 mm and the position 560 mm after compensation, and the positive stroke position 720 mm and the negative stroke position 240 mm exceed the maximum preset error after compensation. It can be seen from **Fig. 9** (b) that the negative stroke position 240 mm and the position 560 mm are both at approximate compensations out of tolerance positions.

In order to briefly describe the compensation process, only the first group of detection data and compensation process are exhibited, and the other four groups of detection data and compensation process are omitted. However, the methods involved are consistent. The remaining four groups of measurement data are analyzed according to the above method, and the compensation results are shown in **Fig. 11**.

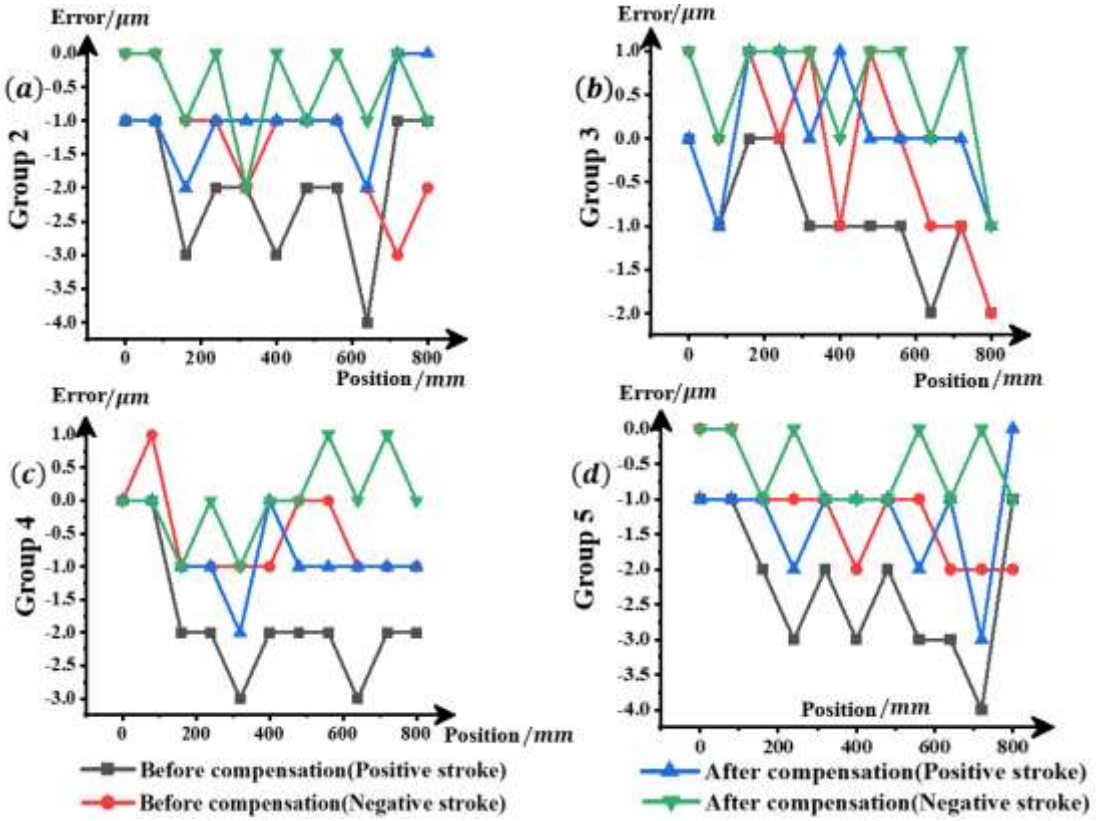

Fig. 11. Error comparison before and after compensation model application

It can be seen from **Fig. 11** that the error fluctuation is significantly reduced after compensation. There are 88 sets of data in the rest four groups of experiments, and the compensation command is started for 60 times. A total of 121 μm errors were found in the original data. After compensation, the total error was reduced by 114 μm, accounting for 94% of the reduced error. The error increased by 4 μm, accounting for 3% of the increased error. The size of the error of 3 μm remained unchanged, but the direction changed. After compensation, a total of 6 groups of data exceeds the maximum preset error, and the error rate accounts for 7%.

According to the definition of calculating the repeated positioning error of the linear axis in the international standard ISO230-2, the repeated positioning error before and after compensation is calculated respectively based on the above five groups of measured data and compensated data. The calculation process is as follows.

The feed shaft moves back and forth for five times in a certain direction, and the error $X_{i,j}$ of the jth movement to P_i is

$$X_{i,j} = P_{i,j} - P_i \tag{4}$$

Where $P_{i,j}$ are the actual arrival position of the feed axis, and P_i is the target position of the feed axis.

Average position deviation X_{ave_i} of feed axis at P_i is

$$X_{ave\_i} = \frac{1}{5}\sum_{j=1}^{5} X_{i,j} \tag{5}$$

The reverse clearance B_i at position P_i is

$$B_i = X_{ave\_i}\uparrow - X_{ave\_i}\downarrow \tag{6}$$

Among them, the symbol ↑ represents positive motion and ↓ represents negative motion.

The unidirectional standard uncertainty S_i of the position P_i is further obtained as

$$S_i \uparrow = \sqrt{\frac{1}{4}\sum_{j=1}^{5}\left(X_{i,j} \uparrow - X_{ave\_i} \uparrow\right)^2} \tag{7}$$

$$S_i \downarrow = \sqrt{\frac{1}{4}\sum_{j=1}^{5}\left(X_{i,j} \downarrow - X_{ave_i} \downarrow\right)^2} \tag{8}$$

The unidirectional repeated positioning error R_i at position P_i is

$$R_i \uparrow = 4S_i \uparrow \tag{9}$$

$$R_i \downarrow = 4S_i \downarrow \tag{10}$$

Finally, the bi-directional repeated positioning error R at position P_i is obtained as

$$R = max\{R_i \uparrow, R_i \downarrow, 2S_i \uparrow + 2S_i \downarrow + |B_i|\} \tag{11}$$

The repeated positioning error of each point of the feed axis before and after compensation is shown in **Fig. 12**.

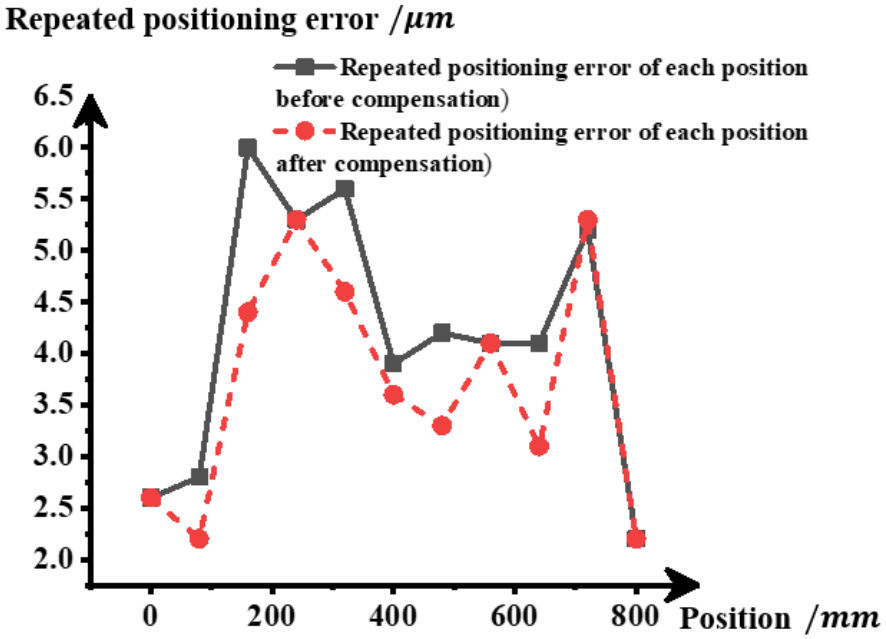

Fig. 12. Comparison of repeated positioning errors at various positions before and after compensation

It can be seen from **Fig. 12** that the repeated positioning error after compensation is generally lower than that before compensation. The compensation effect of different positions is also significantly different, among which 160 mm, 480 mm and 640 mm positions have the most apparent compensation effect and reduce the repeated positioning error by more than 1 μm. The main reason for t this difference is that the error digital map obtained at different positions is different, combined with the control of the maximum preset error and out of tolerance probability, resulting in different amplitude and direction of different position compensation.

Conclusions

The difficulty to tackle this error is rooted in the randomness of repeated positioning error. In the past, the repeated positioning error suppression method of feed shaft is mainly to adjust the assembly sequence repeatedly. This method is characterized by blindness and tendency to damage part. In view of the above problems, the probability compensation research of repeated positioning error is carried out. Combined with the random distribution characteristics of error and dynamic optimization algorithm, the ideal error of different positions is determined in the form of probability,

and further compensation is conducted. Based on the results and analysis, the following conclusions can be drawn:

(1) A description method of repeated positioning error of feed shaft is proposed. Based on a large number of random errors, we draw a digital map of repeated positioning errors. With the error and probability as coordinates, the possibility of each error is displayed, which lays a data basis for error compensation;

(2) The probability compensation model of repeated positioning error of feed shaft is constructed. We extract the digital map and use the dynamic optimization algorithm to search the peak value and its coordinates of the map. Furthermore, we determine the size and direction of the compensation value according to the actual compensation demand;

(3) A dynamic modeling method of probability compensation model for repeated positioning error is described. We build a digital map model base in which new errors automatically participate in digital map rendering and update the map base in real time, thus realizing the dynamic update of the model.

Statements and Declarations

Competing Interests

The authors declare that they have no known competing financial interests or personal relationships that could have appeared to influence the work reported in this paper.

Funding

This research is supported by Jiangsu Science and Technology Achievement Conversion Project (No.BA2018093).

References

[1] Altintas Y, Verl A, Brecher C, et al. Machine tool feed drives[J]. CIRP Annals - Manufacturing Technology, 2011, 60(2):779-796.

[2] Li T, Zhao C and Zhang Y. Adaptive on-line compensation model on positioning error of ball screw feed drive systems used in computerized numerical controlled machine tools. Proc IMechE, Part B: J Engineering Manufacture, 2019, 233: 914–926.

[3] Chen G, Sun Y, An C, et al. Measurement and analysis for frequency domain error of ultra-precision spindle in a fly cutting machine tool. Proc IMechE, Part B: J Engineering Manufacture, 2018, 232(9): 1501–1507.

[4] Guangming, Sun, Gaiyun, et al. Experimental study on the repeatability of positioning of linear axes of machine tools: [J]. Proceedings of the Institution of Mechanical Engineers, Part B: Journal of Engineering Manufacture, 2019, 234(4):739-751.

[5] Szipka K, Archenti A. Utilization of Multi-Axis Positioning Repeatability Performance in Kinematic Modelling[J]. International Journal of Automation Technology, 2019, 13(1):149-156.

[6] Mori M, Ota K, Matsubara A, et al. Design and formation of workforce skills for machine tool assembly. CIRP Annals - Manufacturing Technology, 2015, 64(1): 459–462.

[7] Lu C, Wang S L. An approach to evaluating product assembly precision considering the effect of joint surface deformation[J]. ARCHIVE Proceedings of the Institution of Mechanical Engineers Part C Journal of Mechanical Engineering Science 1989-1996 (vols 203-210), 2014, 228(14):2604-2617.

[8] Sun Y, Wang D, Dong H, et al. Pre-deformation for Assembly Performance of Machine Centers[J]. Chin J Mech Eng-En, 2014, 27(3):528-536.
[9] Gaiyun He, Longzhen Guo, Suqian Li, Dawei. Simulation and analysis for accuracy predication and adjustment for machine tool assembly process[J]. Advances in Mechanical Engineering (Sage Publications Inc.), 2017, 9(11): 168781401773447.
[10] Guangming Sun, Gaiyun He, Dawei Zhang, et al. Effects of geometrical errors of guideways on the repeatability of positioning of linear axes of machine tools[J]. International Journal of Advanced Manufacturing Technology, 2018, 98(9-12):2319-2333.
[11] Shang P, Gao C, Han Z, et al. Simulation Study on Thermal Balance-Temperature Rise Characteristics of a Precision Ball Screw-Nut Pair[J]. Journal of Tianjin University (Science and Technology), 2019,57(7):725-732.
[12] Zhu J, Ni J, Shih A J. Robust machine tool thermal error modeling through thermal mode concept[J]. Journal of Manufacturing Science and Engineering, Transactions of the ASME, 2008, 130(6):0610061-0610069.
[13] Yang H, Ni J. Dynamic neural network modeling for nonlinear，nonstationary machine tool thermally induced error[J]. International Journal of Machine Tools and
Manufacture, 2005, 45(4-5):455-465.
[14] Zhang J, Li B, Zhou C, et al. Positioning error prediction and compensation of ball screw feed drive system with different mounting conditions[J]. Proceedings of The Institution of Mechanical Engineers Part B-Journal of Engineering Manufacture，2016, 230(12):2307-2311.
[15] Shi H, Ma C, Yang J, et al. Investigation into effect of thermal expansion on thermally induced error of ball screw feed drive system of precision machine tools[J].
International Journal of Machine Tools & Manufacture, 2015, 97:60-71.
[16] Liu W, Zhang Y, Fang H, et al. Assembly Method and Assembly Error Evaluation of Machine Tool Linear Rolling Guide Pair[J]. Mechanical Engineer, 2018(08):74-76.